J|A|C|S
ARTICLES
Published on Web 03/15/2006

Tandem Chain Walking Polymerization and Atom Transfer Radical Polymerization for Efficient Synthesis of Dendritic Nanoparticles for Bioconjugation

Guanghui Chen,[†] Devan Huynh,[‡] Philip L. Felgner,[‡] and Zhibin Guan*,[†]

Contribution from the Department of Chemistry, 516 Rowland Hall, and the Center for Virus Research, 3421 McGaugh Hall, University of California, Irvine, California 92697-2025

Received October 29, 2005; Revised Manuscript Received February 11, 2006; E-mail: zguan@uci.edu

Abstract: A tandem polymerization methodology, chain walking polymerization (CWP) followed by atom transfer radical polymerization, was developed for efficient synthesis of nanoparticles for bioconjugation. Using the chain walking palladium-α-diimine catalyst (catalyst **1**), dendritic polymers bearing multiple initiation sites were synthesized and used as macroinitiators for subsequent Cu(I)-mediated ATRP. Control of molecular weight and size of the water-soluble core−shell polymeric nanoparticles was achieved by tuning reaction conditions. Addition of an *N*-acryloyloxysuccinamide (NAS) monomer at the end of the ATRP afforded NHS-activated polymer nanoparticles. Conjugation with both small dye molecules and protein (ovalbumin) yielded nanoparticle conjugates with relatively high dye or protein per particle ratio. With the efficient synthesis and good biocompatibility, these nanoparticles may find many potential applications in bioconjugation.

Introduction

Nanoparticle−biomolecule conjugates are actively investigated for various nanobiotechnology applications including catalysis, sensors, bioanalysis, drug delivery, and bioelectronics.[1] In parallel to the development of inorganic nanoparticles for these applications, organic nanostructures have received increasing attention recently because in principle organic synthesis can provide more precise control over the molecular structure, size, and functionality of nanostructures.[2−5] Among others, nanoparticles based on dendritic macromolecules are especially attractive because they have a globular shape in solution with molecular dimensions right in the nanometer range.[6,7] However, the difficulty of preparing dendrimers through stepwise synthesis and the ultimate size limit for regular dendrimers warrant the search for more efficient methodologies for constructing dendritic nanoparticles. In the current study, we combined two powerful transition-metal-catalyzed polymerization methods, chain walking polymerization (CWP) followed by atom transfer radical polymerization (ATRP), to efficiently synthesize dendritic nanoparticles with tunable sizes and reactive surface functionalities. To the best of our knowledge, this is the first example of tandem catalytic coordination/living radical polymerization for constructing polymer nanoparticles.[8,9]

Our previous studies have shown that CWP provides efficient control of polymer topology.[10−13] Linear, hyperbranched, and dendritic copolymers containing a range of functionalities were obtained by CWP of simple olefinic monomers. In addition, we recently succeeded in a facile synthesis of core−shell dendritic polymeric amphiphiles that behave as unimolecular micelles in water.[13] Despite its efficiency, this approach has a few limitations: (1) the size of the nanoparticle is relatively small, as it is limited by the length of available heterodifunctionalized poly(ethyeleneglycol) (PEG); (2) multistep functionalization of PEG chain ends is tedious and inefficient, and (3) the approach is not general for other types of shell structures. ATRP has evolved into a major living/controlled radical polymerization method for precision polymer synthesis.[14] To overcome the limitations described above, herein we combined two powerful transition-metal-catalyzed polymerization methods to develop a tandem CWP−ATRP approach as a general and efficient methodology for constructing dendritic nanoparticles with controllable size and reactive surface functionalities that are ready for bioconjugation.

[†] Department of Chemistry.
[‡] Center for Virus Research.

(1) Katz, E.; Willner, I. *Angew. Chem., Int. Ed.* **2004**, *43*, 6042−6108 and references therein.
(2) Grimsdale, A. C.; Müllen, K. *Angew. Chem., Int. Ed.* **2005**, *44*, 5592−5629.
(3) Moore, J. S. *Acc. Chem. Res.* **1997**, *30*, 402−413.
(4) Rolland, J. P.; Maynor, B. W.; Euliss, L. E.; Exner, A. E.; Denison, G. M.; DeSimone, J. M. *J. Am. Chem. Soc.* **2005**, *127*, 10096−10100.
(5) Qi, K.; Ma, Q.; Remsen, E. E.; Clark, G. C., Jr.; Wooley, L. K. *J. Am. Chem. Soc.* **2004**, *126*, 6599−6607.
(6) *Dendrimers and Other Dendritic Polymers*; Frechet, J. M. J., Tomalia, D., Eds.; John Wiley & Sons Ltd.: Hoboken, NJ, 2001.
(7) Kramer, M.; Stumbe, J.-F.; Turk, H.; Krause, S.; Komp, A.; Delineau, L.; Prokhorova, S.; Kautz, H.; Haag, R. *Angew. Chem., Int. Ed.* **2002**, *41*, 4252−4256.
(8) Wasilke, J.-C.; Obrey, S. J.; Baker, R. T.; Bazan, G. C. *Chem. Rev.* **2005**, *105*, 1001−1020.
(9) Kolb, L.; Monteil, V.; Thomann, R.; Mecking, S. *Angew. Chem., Int. Ed.* **2005**, *44*, 429−432.
(10) Guan, Z.; Cotts, P. M.; McCord, E. F.; McLain, S. J. *Science* **1999**, *283*, 2059−2062.
(11) Guan, Z. *J. Polym. Sci., Part A: Polym. Chem.* **2003**, *41*, 3680−3692.
(12) Chen, G.; Ma, X. S.; Guan, Z. *J. Am. Chem. Soc.* **2003**, *125*, 6697−6704.
(13) Chen, G.; Guan, Z. *J. Am. Chem. Soc.* **2004**, *126*, 2662−2663.
(14) Matyjaszewski, K.; Xia, J. *Chem. Rev.* **2001**, *101* 2921−2990.

10.1021/ja0573864 CCC: $33.50

Scheme 1. Tandem CWP−ATRP for Nanoparticle Synthesis

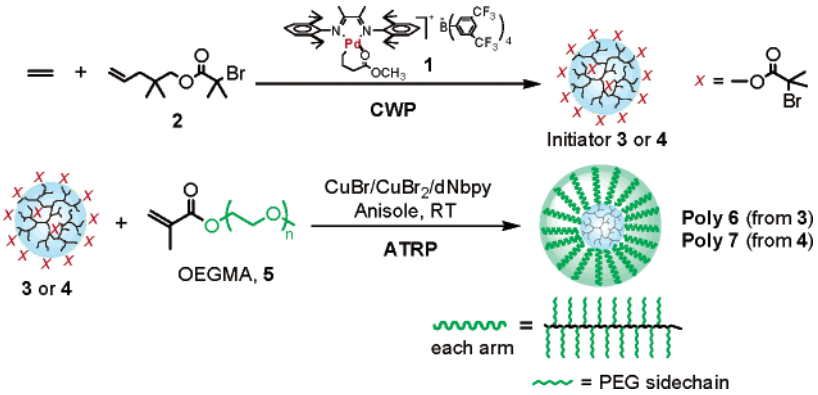

Table 1. SEC and SEC-MALS Characterizations of Initiators and ATRP Polymers

entry	polymer	initiator	time (h)	M_n from SEC[d] (10^3 g/mol)	M_w from SEC[d] (10^3 g/mol))	PDI from SEC	M_n from MALS[e] (10^3 g/mol)	M_w from MALS[e] (10^3 g/mol)	PDI from MALS	R_g[f] (nm)
1	**3**			88	148	1.6	206	314	1.5	14 ± 2.2
2	**4**			53	88	1.6	124	192	1.5	11 ± 3.0
3[a]	**6-1**	**3**	1	149	255	1.6	610	940	1.5	19.2 ± 2.0
4[a]	**6-2**	**3**	2	198	324	1.6	1023	1407	1.4	21.5 ± 1.9
5[a]	**6-3**	**3**	4	279	431	1.5	1894	2646	1.4	27.7 ± 1.7
6[a]	**6-4**	**3**	6	328	505	1.5	2669	3870	1.4	32.9 ± 1.6
7[a]	**6-5**	**3**	8	346	558	1.6	3449	4961	1.4	37.3 ± 1.3
8[a]	**6-6**	**3**	13	391	606	1.5	5096	7302	1.4	45.5 ± 1.2
9[a]	**6-7**	**3**	24	435	669	1.5	7040	9430	1.3	55.3 ± 1.1
10[a]	**6-8**	**3**	48	463	708	1.5	8500	10440	1.2	61.8 ± 0.6
11[a]	**6-9**	**3**	72	478	737	1.5	9180	10980	1.2	64.0 ± 0.5
12[b]	**7-1**	**4**	1	97	157	1.6	344	533	1.5	15.2 ± 2.3
13[b]	**7-2**	**4**	2	135	213	1.6	543	798	1.4	17.0 ± 2.1
14[b]	**7-3**	**4**	4	195	310	1.6	995	1373	1.4	20.5 ± 2.0
15[b]	**7-4**	**4**	6	238	368	1.5	1350	1957	1.4	25.4 ± 1.8
16[b]	**7-5**	**4**	8	271	417	1.5	1789	2558	1.4	28.1 ± 1.7
17[b]	**7-6**	**4**	12	321	519	1.5	2560	3609	1.4	33.1 ± 1.4
18[c]	**9**	**3**	36[g]	289	465	1.5	2078	2634	1.3	27.9 ± 1.5

[a] Reaction conditions: initiator **3**, [$COC(CH_3)Br$] = 8 mM, [Cu(I)] = 16 mM, [Cu(II)] = 1.6 mM, [dNbpy] = 35.2 mM, [M] = 0.5 M, solvent: anisole, room temperature. [b] Reaction conditions: initiator **4**, [$COC(CH_3)Br$] = 8 mM, [Cu(I)] = 16 mM, [Cu(II)] = 1.6 mM, [dNbpy] = 35.2 mM, [M] = 0.5 M, solvent: anisole, room temperature. [c] Reaction conditions: initiator **3**, [$COC(CH_3)Br$] = 8 mM, [Cu(I)] = 16 mM, [Cu(II)] = 1.6 mM, [dNbpy] = 35.2 mM, [M] = 0.5 M, [NAS] = 0.1 M, solvent: anisole, room temperature. [d] Data based on SEC calibration using linear polystyrene standards (Aldrich). [e] Data based on SEC-MALS. [f] Weight average radius of gyration. [g] Reaction time is 12 h + an additional 24 h after addition of NAS.

Results and Discussion

Macroinitiators Synthesis. As shown in Scheme 1, the tandem polymerizations were carried out in two steps. In the first step, dendritic macroinitiators bearing many radical initiation sites on chain ends were synthesized through copolymerization of ethylene and comonomer **2** using the chain walking palladium-α-diimine catalyst[15] under conditions reported previously.[13] By varying CWP conditions, we prepared two dendritic macroinitiators for this study: initiator **3** with a number-averaged molecular weight (M_n, measured by size exclusion chromatography using a multiangle light scattering detector (SEC-MALS)) of 206 000 g/mol and 538 initiation sites (*x* groups) and initiator **4** with a M_n of 124 000 g/mol and 357 initiation sites. The relative molecular weight data for **3** and **4** were obtained by regular SEC using polystyrene standards. The absolute molecular weight and molecular size (radius of gyration, R_g) were measured by SEC-MALS (entries 1 and 2 in Table 1). Consistent with the dendritic topology, the relative molecular weight values obtained by regular SEC are significantly smaller than the absolute values measured by MALS. The number of initiation groups in the initiators was calculated from their corresponding NMR spectra (see Supporting Information for details).

ATRP with the Macroinitiators. In the second step, the dendritic macroinitiators (**3** and **4**) were used to initiate ATRP polymerizations to form core−shell polymers. We chose an oligo(ethylenegylcol) methacrylate (OEGMA, M_n = 300) as the comonomer for the ATRP to provide both water solubility and biocompatibility for the final nanoparticles. Following reported conditions,[16,17] ATRP was carried out at room temperature with a $CuBr/CuBr_2$/dNbpy (molar ratio of 1:0.1:2.2) catalyst system. The low polymerization temperature and the addition of a small amount of $CuBr_2$ were to ensure very low stationary radical concentration on each dendritic polymer and, hence, to suppress intra- and intermolecular radical coupling reactions.[16,17] Our ATRP condition optimization indicated that a ratio of CuBr/initiator of 2:1 afforded the best control of the polymerization. Presumably, the excess amount of the catalyst could compensate partial loss of Cu(I) during the relatively long polymerization period.

A series of amphiphilic core−shell copolymers were prepared by ATRP of OEGMA using dendritic macroinitiators **3** (entries

(15) Johnson, L. K.; Killian, C. M.; Brookhart, M. *J. Am. Chem. Soc.* **1995**, *117*, 6414−6415.
(16) Sumerlin, B. S.; Neugebauer, D.; Matyjaszewski, K. *Macromolecules* **2005**, *38*, 702−708.
(17) von Werne, T.; Patten, T. E. *J. Am. Chem. Soc.* **2001**, *123*, 7497−7505.

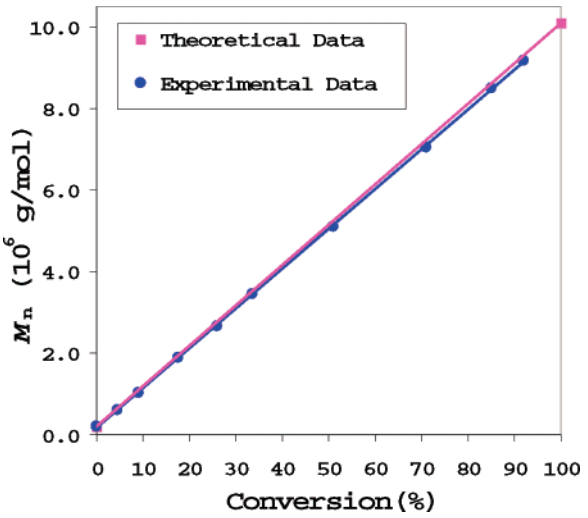

Figure 1. M_n vs conversion of polymerization using macroinitiator **3**; M_n was obtained from SEC-MALS. Reaction conditions: [COC(CH$_3$)Br] = 8 mM, [Cu(I)] = 16 mM, [Cu(II)] = 1.6 mM, [dNbpy] = 35.2 mM, [M] = 0.5 M, solvent = anisole, reaction temperature of 25 °C.

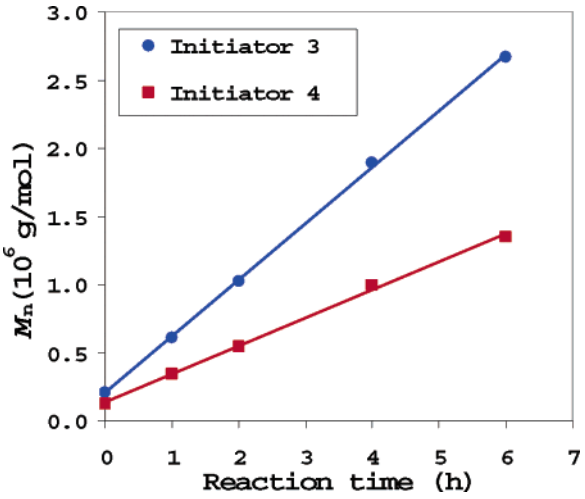

Figure 2. M_n vs reaction time in two polymerization reactions with initiator **3** (M_n = 206 000 g/mol) and initiator **4** (M_n = 124 000 g/mol). M_n was obtained from SEC-MALS. Reaction conditions for both polymerizations: [COC(CH$_3$)Br] = 8 mM, [Cu(I)] = 16 mM, [Cu(II)] = 1.6 mM, [dNbpy] = 35.2 mM, [M] = 0.5 M, solvent = anisole, reaction temperature of 25 °C.

3−11 in Table 1) and **4** (entries 12−17 in Table 1). The molecular weight and molecular size data for the core−shell copolymers increased with the ATRP time. (Table 1, entries 3−17). Again, consistent with the dendritic core−shell topology, the relative molecular weight values obtained by regular SEC are much smaller than the absolute values measured by MALS. As expected from the radial growth, this discrepancy increases with the growth of the final polymer size.

ATRP proceeded in a controlled fashion as evidenced by the linear growth of M_n of the dendritic polymers with the monomer conversion (Figure 1). Simply by controlling the polymerization time, a series of polymers (**6-1** to **6-9** in Table 1) were obtained in gram quantities with a broad range of molecular weights and sizes (from M_n = 610 000 g/mol and a radius of gyration R_g = 19.2 nm to M_n = 9 180 000 g/mol and R_g = 64 nm). On the basis of the conversions, theoretical values of the number-averaged molecular weight are also shown in Figure 1, which correlate well with the experimental data. At relatively low monomer conversions, the polymerization follows pseudo-zero-order kinetics and the M_n of the polymers increases linearly with reaction time (up to 8 h, Figure 2), which provided us a very convenient method to control the molecular weight and size for the final polymer nanoparticle.

Functional Nanoparticle Synthesis. To introduce reactive groups to the dendritic nanoparticles for further bioconjugation, an acrylate comonomer containing an *N*-hydroxysuccinamide (NHS) group, *N*-acryloyloxysuccinamide (NAS, **8**), was used to cap the end of the polymer arms. This methodology is based on the fact that the addition of an acrylate monomer will generate a more stable secondary C−Br bond which is significantly less reactive for further polymerization. This essentially "caps" each methacrylate chain end with an acrylate unit (NAS).[18] For example, after 12 h of OEGMA polymerization using macroinitiator **3**, an NAS comonomer was added and the polymerization was allowed to continue for another 24 h (Scheme 2). Scaffold **9** was obtained after dialysis which has a M_n of 2 078 000 g/mol and a R_g of 27.9 nm (entry 18 in Table 1). From the ^{1}H NMR spectrum, it was calculated that 49% of the chain ends in scaffold **9** are converted to NHS-activated ester groups.

Hydrodynamic Characterization of Scaffold 9 in Aqueous Solution. Dynamic light scattering measurements of scaffold **9** in PBS buffer solution were performed using a Dawn EOS 18-angle light scattering detector (laser wavelength of λ = 690 nm) coupled with a QELS detector (Wyatt Technology Corporation, Santa Barbara, CA). The measurements were done using batch mode at a scaffold concentration of 1 mg/mL in PBS buffer solutions at 25 °C. The average hydrodynamic radius, R_h, of scaffold **9** in PBS buffer solution was measured to be 52 ± 2 nm by dynamic light scattering.

Conjugation of Scaffold 9 with Fluorescein Dye. To investigate the reactivity and availability of the NHS group on the prepared nanoparticles, a derivative (**10**) of a common dye molecule fluorescein was used in our initial conjugation studies. The protein mimic dye molecule **10** was prepared by following a literature-reported procedure[19] (Scheme 3). The molar absorptivity (ϵ) of **10** was determined from Beer's law to be 51 300 $M^{-1}cm^{-1}$ (see Supporting Information, Figures S1 and S2).

Scaffold **9** (1 μM) was incubated in a PBS buffer solution of **10** (pH 8.5, 1 mM) at 4 °C for 12 h, followed by dialysis against water (molecular weight cutoff (MWCO) of dialysis tube is 10 000 g/mol) (Scheme 4). Conjugate **11** was obtained as bright yellow oil (UV/vis and fluorescence spectra of **11** are in the Supporting Information, Figures S3 and S4). Calculated from its absorbance, the average number of dye molecules per polymer scaffold in F-conjugate **11** is 136, indicating that about 50% of the NHS groups were conjugated to the dye.

Conjugation of Scaffold 9 with Ovalbumin. Ovalbumin, one of the most commonly used proteins, was chosen for our protein conjugation studies. Ovalbumin is relatively small (M_w = 44 287 g/mol) compared to scaffold **9** (M_n = 2 078 000 g/mol). Conjugation of ovalbumin to **9** was conducted at

(18) Bon, A. F. S.; Steward, A. G.; Haddleton, D. M. *J. Polym. Sci., Part A: Polym. Chem.* **2000**, *38*, 2678−2686.

(19) Trevisiol, E.; Defrancq, E.; Lhomme, J.; Laayounb, A.; Cros, P. *Tetrahedron* **2000**, *56*, 6501−6510.

Scheme 2. Synthesis of Functional Nanoparticles

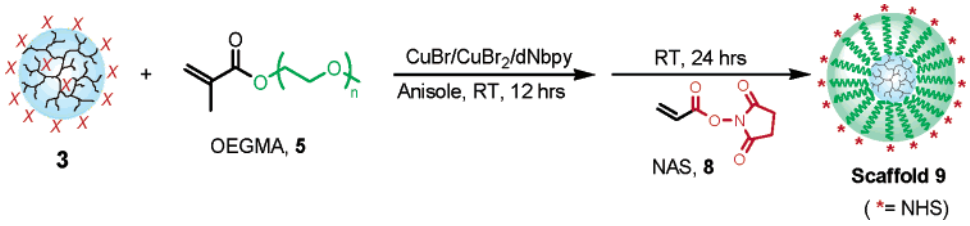

Scheme 3. Synthesis of Fluorescein Derivative **10**

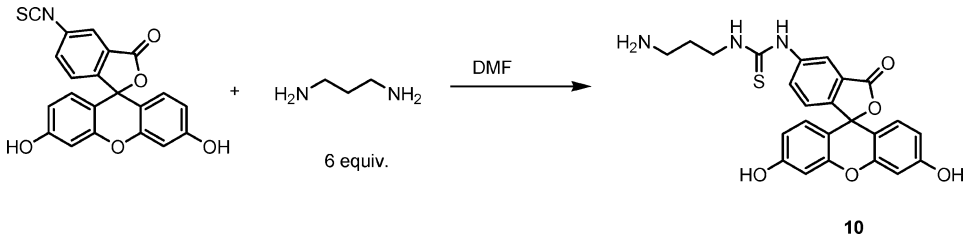

Scheme 4. Synthesis of Fluorecein Conjugate **11**

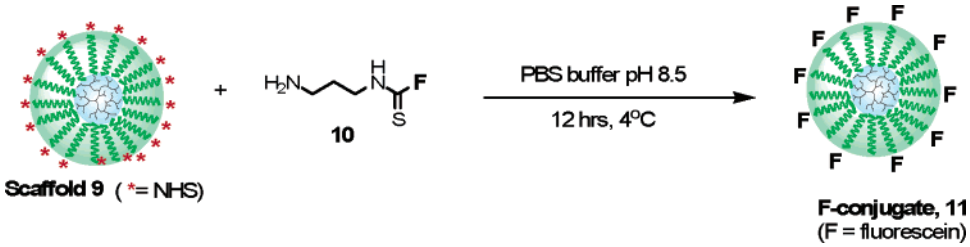

Scheme 5. Synthesis of OB Conjugate **12**

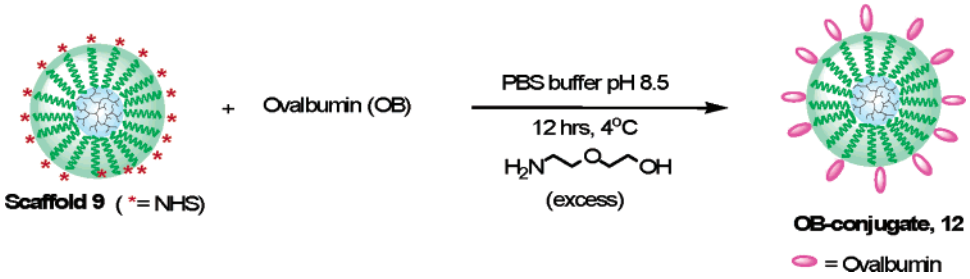

conditions similar to those for the preparation of **11** (ratios of protein to scaffold: weight ratio = 1:1, molar ratio = 47:1). At the end of the reaction, an excess amount (10 equiv) of amino-diethyleneglycol was added to quench any remaining NHS activated chain ends (Scheme 5).

The crude reaction solution was subjected to SEC to confirm the formation of OB conjugate **12**. Figure 3 compares the SEC traces of the conjugation solution, free ovalbumin, and free scaffold **9**, respectively. The shift of UV absorbance at 280 nm indicated that the majority of ovalbumin was conjugated to the nanoparticle scaffold. Integration of the SEC curve shows that 84% of the ovalbumin exists as the conjugated form and 16% exists as the free ovalbumin form. The Bradford assay[20] was also used to obtain the protein concentration of each fraction, from which the amount of protein conjugated to the scaffold was estimated to be 83%, a value agreeing with the SEC result. This relatively high conjugation efficiency indicates the effectiveness of using our core−shell nanoparticles as scaffolds for bioconjugation applications. On the basis of the quantity of scaffold and the amount of conjugated proteins, the number of proteins per scaffold was determined to be 40 in OB conjugate **12**.

We also ran ovalbumin conjugation reactions at an increased protein/scaffold ratio. At a higher protein/scaffold ratio, although

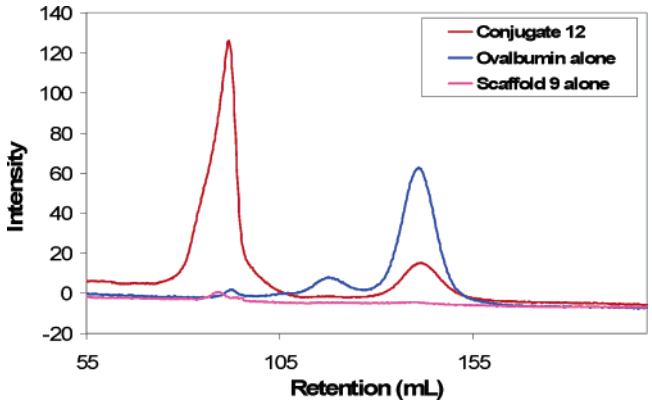

Figure 3. Overlay of SEC chromatograms of OB conjugate **12** crude solution (red), scaffold **9** (magenta), and ovalbumin alone (blue). Mobile phase: 1 × PBS buffer pH 7.4 at 1 mL/min. Absorbance was monitored at a wavelength of 280 nm.

(20) Bradford, M. M. *Anal. Biochem.* **1976**, *72*, 248−254.

the total number of proteins conjugated to one scaffold increased, the overall protein conjugation efficiency decreased. For example, when the protein/scaffold ratio was doubled (i.e., 94:1), the number of proteins conjugated per scaffold was increased from 40 to 49, which means only 52% of the protein was conjugated to the scaffold. A number of factors may limit the maximum number of proteins that can be conjugated to one scaffold. First, the steric repulsion between conjugated proteins may prevent further conjugation reactions. This effect was observed in a recent study of a different system in which a much higher number of proteins per scaffold was obtained for a significantly smaller protein.[21] Second, proteins usually have multiple nucleophilic functionalities on their surfaces (e.g., ovalbumin carries about 20 surface-exposed lysines) which may result in consumption of multiple NHS groups per protein conjugation. Third, both the conformational flexibility and the structural nonuniformity of the core−shell polymers will make a portion of the NHS groups not accessible for protein conjugation. Regardless of these factors, our results have clearly demonstrated that our core−shell nanoparticles are excellent scaffolds for effective multivalent bioconjugation.

Conclusion

In summary, we have shown the first example of tandem catalytic coordination/living radical polymerization for efficient synthesis of nanoparticles for bioconjugation. Using a chain walking palladium catalyst, dendritic macroinitiators bearing multiple radical initiation sites were prepared which were used subsequently in a Cu(I)-mediated ATRP for synthesizing dendritic polymer nanoparticles. The size for both the core and the shell can be controlled precisely. Addition of an NAS monomer at the end of the ATRP afforded NHS-activated polymer nanoparticles as convenient scaffolds for bioconjugation. Conjugation with both small dye molecules and ovalbumin demonstrated that these nanoparticles are effective for multivalent bioconjugation. Currently, we are preparing nanoparticle conjugates with biologically active proteins for specific biological functions. We are also applying this general methodology to prepare dendritic polymer nanoparticles having other kinds of shell structures.

Acknowledgment. We thank the National Science Foundation (DMR-0135233, Z.G.: CAREER), NIH/NIAID (AI056464 & AI061363), and the Innovation Fund from UCI School of Physical Sciences for partial financial support. Z.G. gratefully acknowledges a Camille Dreyfus Teacher-Scholar Award.

Supporting Information Available: Experimental details for the synthesis, polymerization, and spectroscopic studies (PDF). This information is available free of charge via the Internet at http://pubs.acs.org.

JA0573864

(21) Chen, G. Ph.D. Thesis, University of California, Irvine, CA, 2005.